

12pt

**Analysis of the sea-level variability along the Chinese coast and estimation of the impact of global climate change.**

**Maochang Cui**

Institute of Oceanology, Chinese Academy of Sciences, Quindao, China  
and

**Eduardo Zorita**

Institute of Hydrophysics, GKSS Research Centre, Geesthacht, Germany

June 11, 1997

## **Abstract**

The relationship between Chinese coastal sea level (SL) and the atmospheric circulation at monthly time scales has been examined. A canonical correlation analysis between SL and sea-level pressure (SLP) indicates that the SL variability can be well explained by the intensities of the (seasonal) zonal and meridional circulations. Linear statistical models to hindcast SL from the SLP field reproduce reasonably well the SL evolution in an independent period. These models are used to estimate the contribution of a perturbed atmospheric circulation on coastal SL changes in a climate model experiment forced by the IPCC Scenario A greenhouse-gas emissions from 1940 until 2090. The perturbed atmospheric circulation causes a SL change of a few centimeters at the end of the integration, and its sign depends on location and season.

## **Zusammenfassung**

**Studie über die Variabilität des küstennahen Wasserstandes vor China und Abschätzung der Folgen einer durch den anthropogenen Treibhauseffekts veränderten atmosphärischen Zirkulation.** Die Beziehung zwischen Wasserständen an chinesischen Küstenstationen und der atmosphärischen Zirkulation auf monatlichen Zeitskalen wurde untersucht. Eine kanonische Korrelations-Analyse zeigt, dass die Variabilität der Wasserstände gut aus der Intensität der (saisonalen) zonalen und meridionalen Zirkulation abgeleitet werden kann. Werden Wasserstandswerte mit Hilfe von linearen statistischen Modellen aus dem Luftdruckfeld berechnet, so zeigt sich auch für unabhängige Zeiträume eine gute Übereinstimmung mit den Beobachtungen. Diese Modelle wurden verwendet, um die küstennahen Wasserstandsvariationen abzuschätzen, die sich aus einer veränderten atmosphärischen Zirkulation ergeben, wie sie von einem Klimamodellexperiment mit den Treibhausgas-Emissionen von 1940-2090 entsprechend dem IPCC-Szenario A berechnet wurde. Die veränderte atmosphärische Zirkulation bedingt eine Veränderung von wenigen Zentimetern gegen Ende der Integration, wobei das Vorzeichen von Ort und Saison abhängt.

## 1 Introduction.

Sea level is one important environmental parameter concerning coastal ecosystems, harbor building and seawater transport. It is therefore of special importance to firstly describe and secondly understand the variability of sea level and the processes responsible for its changes along the Chinese coast. It is also of major concern for the climatologist to try to estimate changes in coastal sea-level that may be associated with an increase of greenhouse-gas forcing in the atmosphere in the future. For this purpose climate models are the only tools to derive the details, in terms of spatial resolution and magnitude, of the expected climate change. These models have been used to estimate large-scale changes in sea-level due to changes in the oceanic circulation and the volume expansion of sea-water (Mikolajewitz et al., 1990) and the degree of confidence put in the results at large- scales is growing (IPCC, 1996). Such models are, however, limited in their spacial resolution. Even if the grid, which is used for the discretization of the differential equations, is of the order of several hundred kilometers, does a climate model hardly offer useful information on that nominally minimum spatial scale. The reason for this failure lies in the inadequate representation of subgrid-scale information, as the details of orography or the coastal configuration, an erroneous parametrization of the physical process that occur at sub-grid scales, and in the disruption of the nonlinear energy cascade at the lowest end of the spectral resolution in the atmospheric models (von Storch, 1993). For these reasons, as recognize by the 1995 IPCC report, there exists a large uncertainty in the estimation of the sea-level changes due to modification of the waves, tides and storm climates. Some attempts are now being made to estimate changes in sea-level at local and regional scales by embedding high-resolution regional ocean models into large-scale climate models (Kauker, personal communication), the so called *dynamical downscaling*. But until these models are operative other, more flexible, methods such as statistical downscaling (Storch, 1993) have to be used. Within the statistical downscaling framework, the response of a regional variable, in this case coastal sea-level along the Chinese coast, to large-scale climate forcing is described by a linear model, the parameters of which are fitted using available observations. Once the model has been set up, it can be used to reconstruct past variations of the regional variable if large-scale observations extending longer back into the past are available, or to estimate possible regional changes under a perturbed climate

using the output of climate change experiments with coarse-resolution climate models. The statistical models, therefore, try to model in one step the chain of causes and effects that lead from the monthly mean large-scale circulation through the atmospheric transients and wind-stress, waves, tides, rainfall, etc., to local sea-level anomalies. The local peculiarities are taken into account by fitting their internal parameters to observed data sets. This statistical approach has been already applied to coastal sea-level in the Baltic Sea (Heyen et al., 1996) and at the Japanese Islands (Cui et al., 1995).

For the design of reasonable statistical model, some previous physical reasoning about the physical factors affecting coastal sea-level is required. Three groups of processes may be important in this respect: the geological processes, the regional-scale dynamical processes and the large-scale dynamical processes (see, e.g., Patullo et al., 1955; Lisitzin and Patullo, 1961; Gill and Niiler, 1973; Wyrтки, 1990; NRC, 1990). The geological processes are normally very slow (except in the case of earthquakes) and may be treated as linear, or even absent, on time scales of years or decades. If we subtract the linear trends from the local sea level, these processes will efficiently be filtered out. The volume expansion of sea water and the melting of glaciers due to possible global warming (Warric and Orlemans, 1990), as well as human water pumping activities from the subsoil (Sahagian et al., 1994) are another large-scale, and quite probably slow and linear, factors affecting coastal sea-level. If this effect has already enter into play, it can be also filtered out by detrending the data set. More relevant in this context are the regional scale processes, such the inverse barometric effect of more or less air pressing on the surface of the ocean, the steric effect of the water column being more or less dense (as a consequence of changing temperature and the effects of the regional oceanic and atmospheric circulations. More locally, for instance, near a river- mouth the streamflow of the river will influence the local tide gauge, specially for large rivers such as the Yangtze. Of course, once the influence of the local processes has been estimated, all these effects, geological, large- scale and regional, have to be added up for a complete estimation of possible sea-level changes.

The accuracy with which these regional processes are simulated in present- day climate models (with typical horizontal resolutions of  $5^\circ$ ) varies considerably. The inverse barotropic effect depends only on the large-scale atmospheric pressure and is therefore likely well simulated. The steric effect depends on such regional effects like the cloud cover or the availability of mixing

energy, which is less well described by atmospheric models. The effects of local ocean currents, local coast lines and river streamflows are normally not included in such models.

### **1.1 Possible factors affecting Chinese coastal sea-level variability at monthly time scales.**

The Chinese coast is connected to a broad and shallow land shelf with average water depth of only about 20 m and the typical magnitude of anomalous sea level variations is of the order of 50-100 mm. One important factor for sea-level variability is obviously the effect of wind-stress, either by direct pile-up of water, anomalous Ekman transport, or through the dynamical equilibrium with the Coriolis force acting on currents. Since this effect depends strongly on the coastal topography and momentum flux to the ocean its magnitude is difficult to estimate. The magnitude of the inverse barometer effect has been found to be very nearly the equilibrium response of sea water to atmospheric pressure (Wunsch and Stammer, 1997), namely 1 cm *sim* 1 mb. Typical anomalies of monthly atmospheric pressure are of the order of 2 mb, so that the inverse barometer effect could in principle cause sea-level anomalies of 20 mm. Other factors comprise the volume expansion of water caused by temperature variations. The monthly variability of the water temperature anomalies in the mixed layer is typically of the order of 1° C. Since the volume expansion coefficient of seawater is approximately  $2.5 \times 10^{-4} C^{-1}$  the expected sea-level anomalies caused by the steric effect could be also of the order of 20 mm. These figures are just rough estimations of the relative order of magnitude of the different factors. The sea-level anomalies actually observed are of course the result of the interplay of all them, which presumably depends on the local peculiarities of each gauge station.

### **1.2 Election of the large-scale forcing**

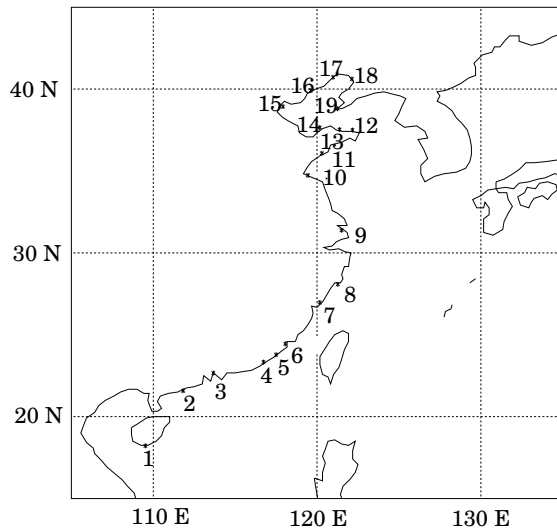
For the formulation of a statistical downscaling model we have to resort to large-scale variables that satisfies two conditions: First, sufficiently long homogeneous time series are available to fit the model the parameters of the statistical model with observed data. Second, the forcing must be well simulated by climate models. The latter condition limits the set of candidates to large-scale or regional-scale fields (with a scale of a couple of thousand kilometers or more), such as sea-surface temperature, sea-level pressure or geopotential height at some level. One has to be

aware, however, of the limitations of such an election. The East Chinese coast is exposed to an important seasonal phenomenon, namely the East Asian Monsoon and its associated intense rainfall. It has been recognized for some time that the summer monsoon always appears first in East Asia, usually in the middle of May, before the Monsoon development over the Bay of Bengal during late May and over the western coast of the Indian subcontinent in early June. In East Asia the earliest onset line occurs in the northern South China Sea, and extends to the western Pacific east of Taiwan and south of Japan. The onset date progresses northward and northwestward. By mid-June the East Asia Monsoon is characterized by the abrupt intensification of rainfall along the Yangtze river and then extending into Japan. The rain-belt moves abruptly into north China in mid-July (Tao and Chen, 1987). About 80% of the total annual precipitation in China falls according to this mean Monsoon evolution. However, the interannual variability is very large (Lau et al., 1988). Therefore it is expected that this phenomenon may exert some influence on the coastal sea-level variability. The reverse situation, i.e. years with anomalously low rainfall should be associated with lower than normal coastal sea-level, at least in the stations located in the basin of large rivers.

It cannot be expected that coarse-resolution climate models be able to simulate properly a phenomenon so complex such as the Monsoon, where the atmospheric circulation, SSTs, topography, and precipitation interact with complicated and not completely understood feedbacks. Statistical models will be able in principle to describe only in a crude way the relationships between SLP and SST in one side, and rainfall and sea-level on the other side. Therefore, the downscaling results in the Monsoon season should be intrinsically considered with more care.

This paper is organized as follows: in section 2 the observational data set used in this study are described. In section 3 the strategy for the formulation of the statistical model is presented. In section 4 the results of the Canonical Correlation Analysis between coastal sea-level and sea-level pressure and sea-surface temperature is analyzed and the validity of the resulting statistical model is tested. In section 5 the downscaling model is applied to interpret the output of a climate change experiment, thus estimating the contribution to future coastal sea-level changes by these forcing fields. The paper is closed with concluding remarks in section 6.

Figure 1: *Positions of the gauge stations used in this study*



## 2 Data.

In this study, we examine monthly mean values of sea level along the Chinese coast, of sea surface temperature and of sea level air-pressure data in the West Pacific and South China Sea and of sea level air-pressure data over China:

- The local sea level data at 19 stations along the Chinese coast for the period January 1960 through December 1990 have been compiled by the Marine Scientific and Technological Data Center at partial coastal stations run by State Oceanic Administration in China. The positions of the 19 tide gauges are given in Fig. 1.
- Fields of monthly sea level pressure over China ( $20^{\circ}\text{N}$ - $50^{\circ}\text{N}$ ,  $80^{\circ}\text{E}$ - $135^{\circ}\text{E}$ ) were available on a  $5^{\circ}\times 5^{\circ}$  grid. Such fields, which have been prepared by the National Center For Atmospheric Research (NCAR) in Boulder, USA, are available for the time interval January 1960 until December 1990.
- For some testing calculations rainfall data were also used. These data were prepared as monthly means gridded field ( $2.5^{\circ}$  longitude  $\times$   $3.5^{\circ}$  latitude over East China ( $20^{\circ}\text{N}$ - $45^{\circ}\text{N}$ ,  $99.5^{\circ}\text{E}$ - $125^{\circ}\text{E}$ ) by the UK Department of Environment for the time interval January 1960-December 1990.

The data have been processed in the following steps.

- Chinese coast is tectonically active. Since 1950's trends of coastal sea-level with different signs have been reported along the Chinese coast (Wang, 1986). The coast near Wusong and Lianyungang rises with a rate of about 5.4 mm/year but the coast in Jiangsu and Shandong Provinces is rather stable and the coast in other regions sinks with a rate of from 8.1 to 10.5 mm/year . It is noticeable that the coast of Tanggu sinks at a rate of up to 46 mm/year after the earthquake in 1976 in Tangsan (Wang, 1986). These rates are estimated mainly from the sea level data itself so that we can not correct the sea level data with these estimates to "clean" the data from tectonic influences. It seems reasonable to assume that these slow tectonic processes that are not directly related to climate, as well as others such as land subsidence by local hydrocarbon mining activities, can be filtered out from the sea-level data by subtracting the long-term linear trend. Since the linear trend can also contain the influence of low-frequency climate variability the climate time series were also detrended for a consistent statistical analysis.
- The anomalies of all data were calculated by subtracting the long- term annual cycle.

### 3 Formulation of the statistical model.

The methodology to specify the statistical model linking coastal sea-level and large-scale climate forcing follows closely the one described by Cui et al. (1995) for the Japanese Islands and heyen et al. (1996) for the Baltic Sea. Therefore, only a brief summary is given here. The anomalies of the large-scale (gridded) forcing  $\vec{L}(t)$  and the response of the local variable  $\vec{R}(t)$  are decomposed in a series of patterns:

$$\begin{aligned}\vec{L}(t) &= \sum_{i=1}^n \alpha_i(t) \vec{p}^i \\ \vec{R}(t) &= \sum_{i=1}^n \beta_i(t) \vec{q}^i\end{aligned}\tag{1}$$

where  $\vec{p}^i$  and  $\vec{q}^i$  are time independent spatial patterns and  $\alpha_i(t)$  and  $\beta_i(t)$  describe the evolution of their amplitudes in time. It is technically convenient to define the time series  $\alpha_i$  and  $\beta_i$  having standard deviation equal to 1. In this way the physical units and the magnitude of the typical anomalies are carried by the spatial patterns.

We use canonical correlation analysis (CCA) to find the optimal decomposition of both fields. The result of CCA are time series  $\alpha_1(t)$  and  $\beta_1(t)$  associated show the highest correlation. The following pair  $\alpha_2(t)$  and  $\beta_2(t)$  shows the highest correlation with the additional constraint that they are uncorrelated with  $\alpha_1(t)$  and  $\beta_1(t)$ , respectively. Lower order pairs are defined in a similar recursive way. The patterns  $\vec{f}^i$  and  $\vec{q}^i$  are called the canonical patterns, the associated time series  $\alpha_i(t)$  and  $\beta_i(t)$  are the canonical time series, and the correlation between them are called the canonical correlations. Therefore, the canonical patterns may be considered to represent optimal associations between both fields and time-uncorrelated processes within each field. For the mathematical details of CCA the reader is referred to Bretherton et al. (1992). The canonical correlation analysis involves the inversion of the covariance matrices of both fields and to avoid numerical instabilities when a large number of grid points is involved, it is convenient to prefilter the data with standard Empirical Orthogonal Function analysis (EOF) and retain only the leading variability modes for the subsequent CCA.

Once the canonical patterns have been found, an estimation of anomalies of the local variables conditional on a given large-scale forcing  $\vec{L}(t_0)$  can be accomplished as follows. The amplitudes of the large-scale canonical patterns and  $\alpha_i(t_0)$  are found by minimizing the error function E:

$$E = \sum_{k=1}^N \left\{ L_k(t_0) - \sum_{i=1}^n (\alpha_i(t_0) p_k^i) \right\}^2 \quad (2)$$

where  $i$  denotes the pattern index and  $k$  indicates the grid- point. The amplitude of regional canonical patterns is estimated simply as:

$$\beta_i(t_0) = c_i \alpha_i(t_0) \quad (3)$$

where  $c_i$  is the  $i^{th}$  canonical correlation. Finally the regional anomalies associated with  $\vec{L}(t_0)$  are estimated as the sum of the contribution of the different canonical patterns:

$$\vec{R}(t_0) = \sum_{i=1}^n \beta_i(t_0) \vec{q}^i = \sum_{i=1}^n c_i \alpha_i(t_0) \vec{q}^i \quad (4)$$

The large-scale forcing  $\vec{L}$  may stem from observations in a validating period or may be simulated by a climate model, therefore allowing for an estimation of local anomalies caused by changes in the large-scale forcing.

## **4 Canonical correlation of sea-level-pressure and coastal sea-level.**

The canonical correlation analysis of sea level variations at the 19 Chinese stations and the sea level pressure anomalies over East Asia China has been performed separately for the winter and summer seasons. The election of the months belonging to each of the half years is based on the importance of the Monsoonal circulation in the area. As explained in the introduction rainfall associated with the East Asian Monsoon starts in May in the South and can be considered to be finished in August-September in the north. Therefore, for this purpose we have defined the summer season as the months May through September, and the winter season as the remaining months.

In both cases the statistical analysis between sea-level and sea-surface temperature (SST) in the western Pacific yielded no clear association, and in any case always weaker than those found between sea-level and atmospheric sea level pressure (SLP). It is known that both fields, SST and SLP, are connected at mid-latitudes, and that the empirical evidence points to a much more active role of the atmospheric anomalies in generating SST anomalies (by air-temperature advection, especially in wintertime, and by Ekman pumping) than in the opposite direction (Lau, 1997). For these reasons the associations between SST and sea-level were not investigated further, since it was assumed that the possible relationships between SST and sea-level through the steric effect would be overshadowed by the direct influence of the atmosphere on sea-level.

### **4.1 Winter half year: October through April**

In winter, two pairs of patterns which are strongly connected (correlations of 0.71 and 0.50), and that represent about 35% and 20% of the total sea-level variance can be identified (Figure 2). The first pattern describes SLP anomalies that are associated with anomalies of the geostrophic wind blowing along the Chinese coast. The coastal sea-level anomalies related to this pattern are negative in the stations located within the Yellow-Sea (see Fig 1) and positive in the rest, exposed to the open ocean. The association between both patterns is physically consistent with water being flushed out from the Yellow sea by the anomalous wind stress and an enhanced Ekman transport into the Chinese coast. The advection of cold air masses from the continent

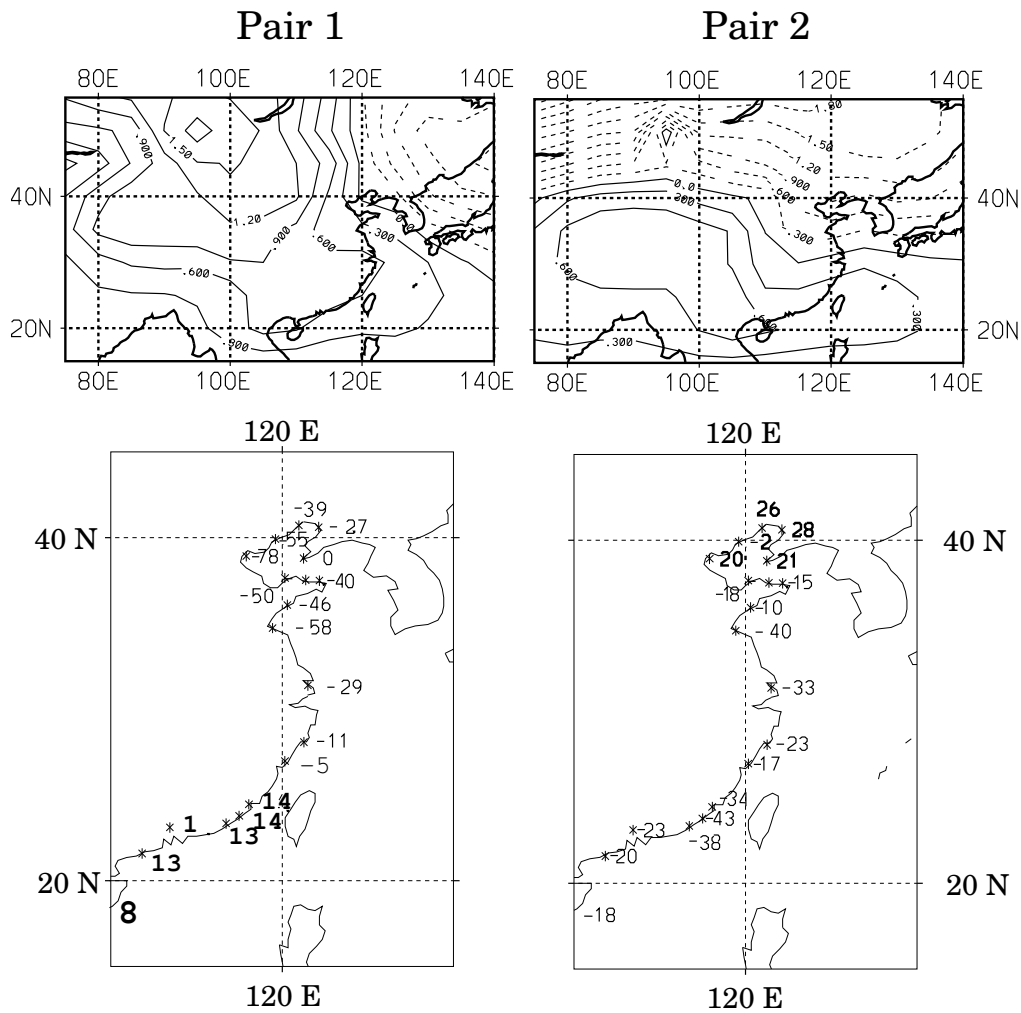
and the subsequent cooling of the Yellow Sea may also contribute, but both effects are difficult to separate in this region. The second SLP pattern shows negative anomalies in the Northwest of China and positive anomalies over much of south and central China. The geostrophic wind anomalies associated with this SLP pattern are directed from the continent to the Pacific Ocean. The sea-level pattern is positive almost everywhere, except in the stations in the Yellow Sea. The most plausible physical explanation for this second pair is the inverse barometer effect. Although there exist dynamical components associated with this effect, at these time scales the relationship between the local SLP and sea-level is quite approximately  $1\text{mb} \sim 1\text{ cm}$  (Wunsch and Stammer, 1997), which agrees reasonably well with the second pair in Figure 2. Other possible mechanisms, such as the steric effect, would yield relationship between SLP and sea-level of the opposite sign as the ones represented by this second canonical pattern. For instance, the SLP pattern is associated with cold air-mass advection from the continent, which should reduce the sea-level in the Yellow Sea.

The validity of the statistical relationship identified by the CCA has been tested by performing the analysis with the data in the period 1960-1975 and trying to reconstruct the sea-level anomalies using the SLP observations in the period 1976-1990, as explained in the previous section, (Eqs. 2-4). The reconstruction is based on the two canonical pairs described previously. The resulting sea-level anomalies in the winter seasons for three representative stations (stations 5, 8 and 12 in figure 1) are shown in Figure 3. One can see that the reconstructed sea-level anomalies agree quite well with the observations for the three stations. This result supports the initial hypothesis that to a great extent the sea-level variability along the whole coast is caused by the direct influence of the atmosphere on the sea-surface.

## **4.2 Summer half year: May through September**

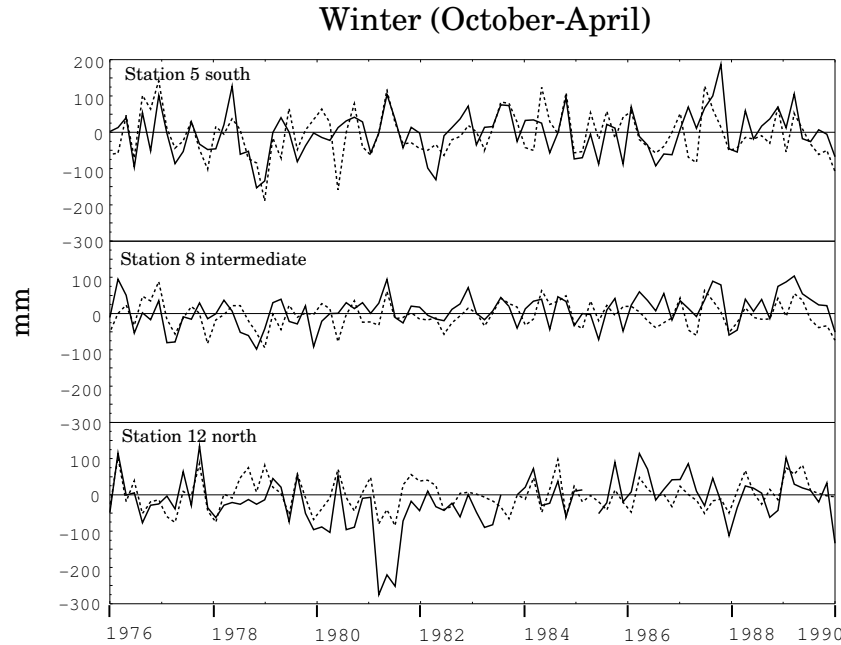
A similar canonical correlation analysis has been performed for the summer months (April-September). The SLP canonical patterns obtained in the summer season (not shown) are different from those in the winter season, as the typical circulation patterns are also different. The first SLP pattern has a north-south dipole structure with a high pressure cell sitting over the Yellow Sea and low pressure over the Western Pacific. The associated geostrophic circulation anomaly is oriented zonally. The second SLP pattern represents a weaker west-east dipole with associ-

Figure 2: *The leading two canonical correlation pairs of SLP (hPa) and sea-level anomalies (mm) in the winter season (October-April). The correlation between the corresponding time series is .71 and .50, respectively. The variance explained by the sea-level patterns is 33% and 19% , respectively.*



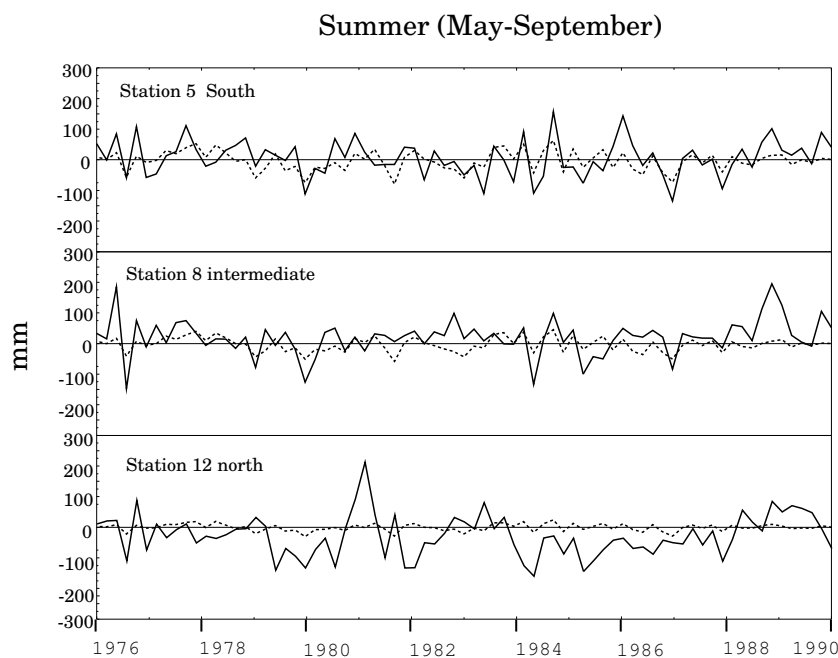
ated meridional geostrophic circulation anomalies. The sea-level variance explained 25% and 12%, respectively. To further investigate the reasons for this low explain variance, the canonical correlation analysis was performed in half of the period available (1960-1975) and the sea-level anomalies in the remaining period (1976-1990) were reconstructed from the SLP observations. The results for the stations 5,8 and 12 are shown in figure 4 . It can be seen that whereas

Figure 3: *Observed (solid) and reconstructed (dashed) monthly sea-level anomalies in stations 5,8,12 (see Fig 1) in winter (October-April). The reconstruction is based on the simultaneously observed SLP anomalies. Units are mm.*



the reconstructed sea-level anomalies agree reasonably well in stations 5 (south) and somewhat worse in station 8 (intermediate), the sea-level reconstruction is very poor in the north (station 12). This suggest that in the summer season the typical patterns of the atmospheric circulation affecting coastal sea-level may be considerably different in the Yellow Sea than in the rest of the Chinese Coast. Therefore, the stations were divided in two groups, the Yellow Sea group (group YS, stations 10-19) and the rest(group R) and the analysis was repeated for two groups separately. The CCA analysis for the group R identifies one just one pair of pattern, shown in 5. The SLP pattern has a dipole structure with negative anomalies over the Western Pacific and positive anomalies over the Yellow Sea. The coastal sea-level anomalies in the China Sea are all positive. This relationship can be reasonably explained by anomalous Ekman upwelling under the low- pressure cell. The CCA of coastal sea-level in the Yellow Sea and SLP is not able to identify any pair of patterns in the summer months that are significantly correlated. However, the EOF analysis of YS sea level indicates that just one single mode is able to describe about

Figure 4: *Observed (solid) and reconstructed (dashed) monthly sea-level anomalies in stations 5,8,12 (see Fig 1) in summer (May-September). The reconstruction is based on the simultaneously observed SLP anomalies and the Canonical Correlation Analysis for all stations simultaneously. Units are mm.*



50 % of variance, having the same sign over all YS stations. Due to the particular characteristics of the coast-line it may be possible that the SLP pattern that forces the sea-level is not contained in the leading EOFs of SLP in this area. To further investigate this hypothesis the regression pattern of the first sea-level principal component and the SLP field was calculated (Fig 6). The SLP describes in fact geostrophic circulation anomalies that should be connected to pile-up of water into the Yellow Sea. This associated SLP pattern is effectively not contained in the subspace spanned by the leading SLP EOFs and actually projects strongly in one of the higher order EOF patterns (not shown). This fact may shed some doubts about the physical significance of this associated SLP pattern and therefore onto the SLP-sea level relationship in the Yellow sea. To ascertain this physical significance we have calculated the regression pattern between the YS sea-level principal component and rainfall in China in the summer season. Our reasoning is that if the associated SLP pattern of figure 6 bears a real physical significance it

Figure 5: *The leading canonical correlation pair of SLP (hPa) and sea-level anomalies (mm) in the Southern stations in the summer season (May-September). The correlation between the corresponding time series is .72 and the variance explained by the sea-level pattern is 45%.*

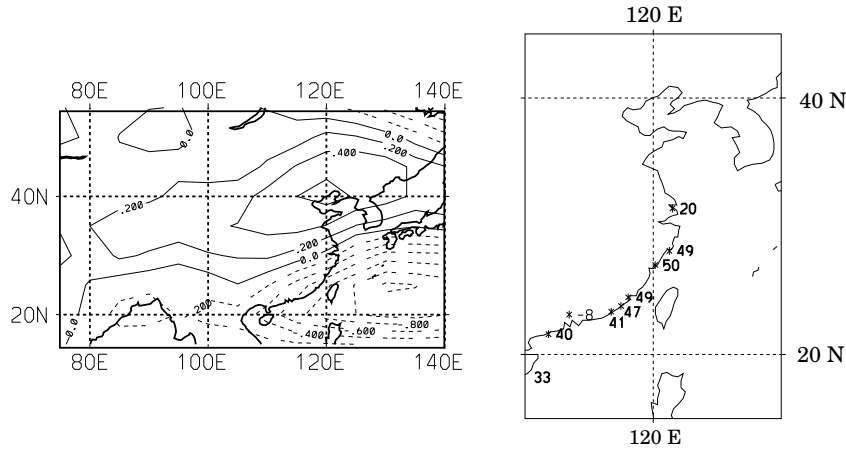
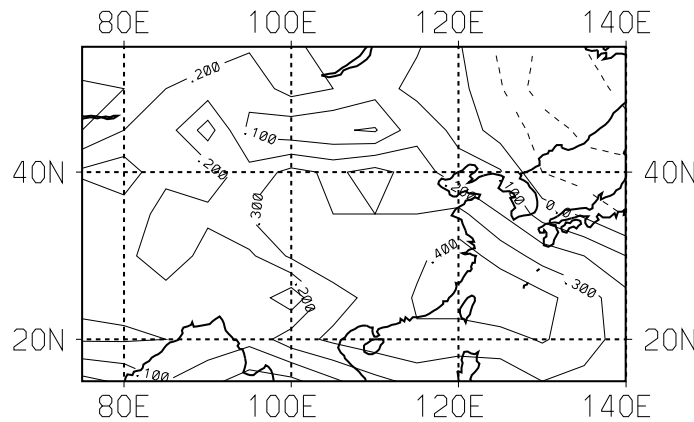


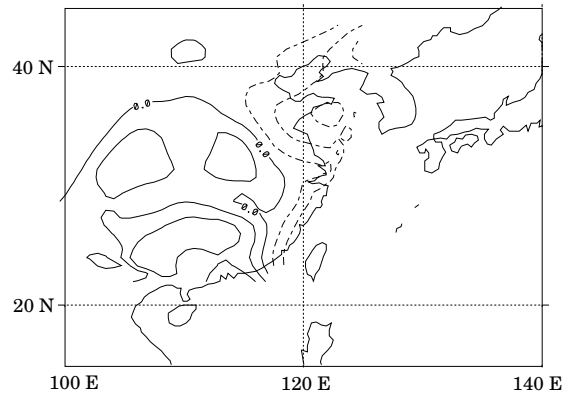
Figure 6: *The SLP regression pattern in the summer season (May-September) based on the first principal component of Yellow Sea coastal sea-level. Units are hPa.*



should also have a fingerprint not only in the YS sea-level, from which it was derived, but also in the rainfall anomalies. This fingerprint should then also appear in the rainfall regression pattern, which is shown in figure 7.

The rainfall regression pattern describes weak positive anomalies in most parts of Central China and South China and positive anomalies along almost the whole East coast and in the

Figure 7: *The rainfall regression pattern in the summer season (May-September) based on the first principal component of Yellow Sea coastal sea-level. Contout interval is 5 cm/month.*



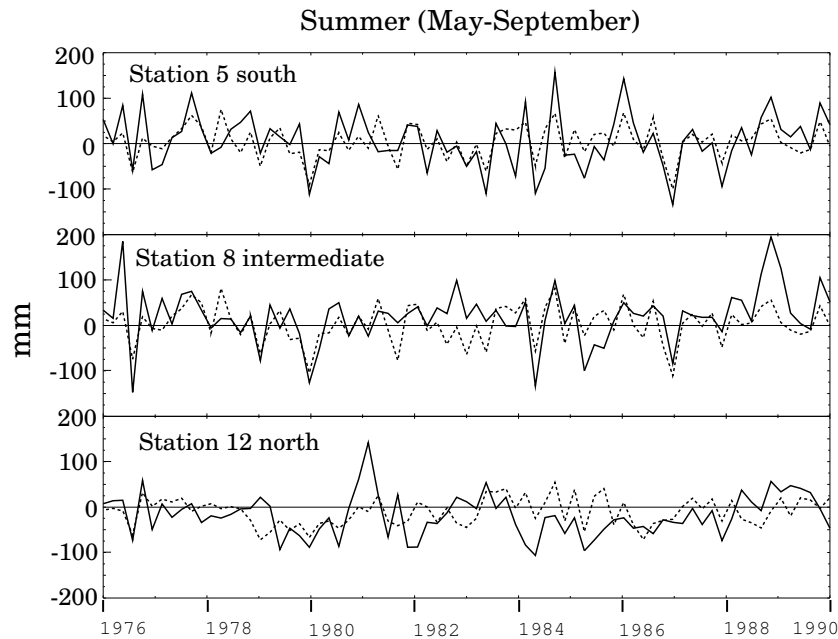
Yellow Sea. One can see that the rainfall regression pattern and the SLP regression pattern in Figure 6 are reasonably physically connected: In summer time the geostrophic wind anomalies should bring moist air masses into the continent, while the high pressure cell sitting at the west coast inhibits the rainfall. This supports the physical existence of the SLP pattern in figure 6 as forcing for the YS sea-level in summer.

The statistical model describing the connection between SLP and coastal sea-level is then separately formulated for the YS stations and for the R stations. For the R group the canonical SLP of figure 5 is taken, while for the Yellow Sea the associated SLP pattern of figure 6 is used. To test the model the same calculations as described in this subsection have been performed for the subperiod 1960-1975, and the corresponding SLP and sea-level patterns have been calculated. The model is then used to reconstruct the sea-level anomalies in summer for the subsequent subperiod 1976-1990. The results for the three representative stations is shown in figure 8.

The agreement between reconstructed and observed sea-level anomalies is now better for all three representative stations, especially in the low frequency variability.

It is concluded that the agreement between observed and reconstructed sea-level anomalies in winter and summer, shown in Figures 3 and 8 lends support to the use of these statistical models to estimate future sea-level changes caused by slow changes of the atmospheric circulation due to anthropogenic greenhouse-gas forcing.

Figure 8: *As in figure 4, but based on a separate statistical model for the Yellow Sea stations and the rest of Chinese stations.*

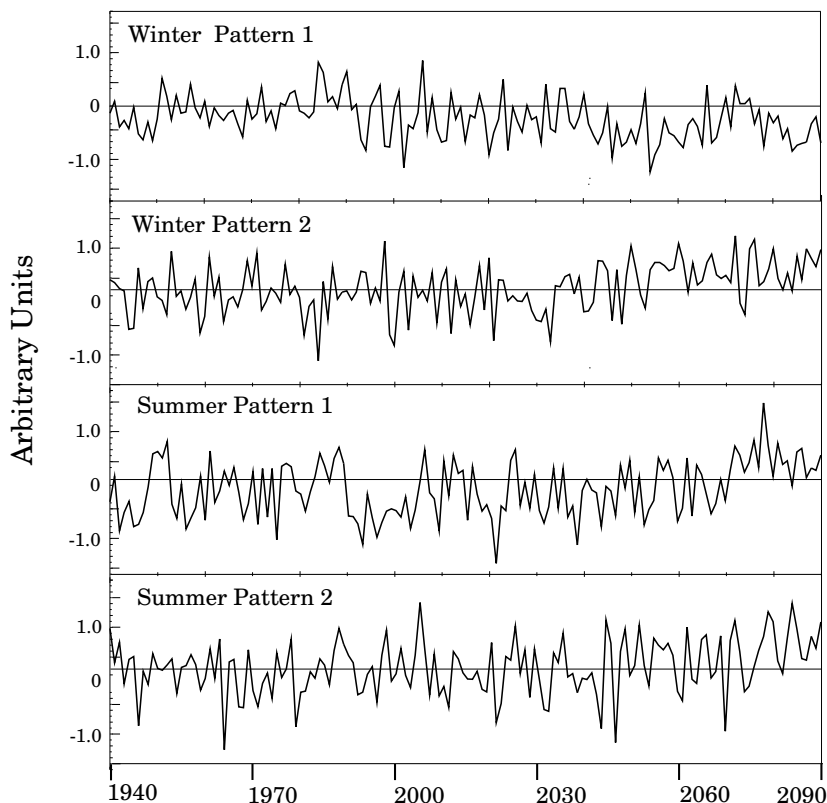


## 5 Estimation of coastal sea-level changes under future anthropogenic greenhouse gas forcing.

The statistical relationship between SLP and coastal sea level can be also used not only to reconstruct past variation of sea-level but also to estimate future changes under different greenhouse forcing scenarios. For this purpose the changes of the atmospheric circulation simulated by a General Circulation Model (GCM) can be used as input for the statistical model. In this section one integration with the ECHAM1-LSG coupled climate will be analyzed. The ECHAM1 atmospheric model is a spectral model with an equivalent horizontal resolution of about  $5.6^\circ$  and 19 levels in the vertical. The LSG ocean model has an effective horizontal resolution of about  $4.2^\circ$  and 11 levels. In this integration the observed concentration of atmospheric greenhouse gases between 1940 and 1985 were prescribed as observed. From 1986 onwards the model was forced by greenhouse gas concentrations according to the Scenario A of the Intergovernmental Panel on Climate Change (IPCC, 1992), which corresponds roughly to a yearly increase of 1% of the

effective CO<sub>2</sub> concentration. The effective CO<sub>2</sub> concentration is therefore doubled at year 2035 of the integration with respect to the concentration in year 1985. Additional details over this coupled climate model can be found in Cubasch et al. (1992) and of this transient experiment in Cubasch et al. (1995). The SLP anomalies from this experiment were calculated by subtracting the *simulated* mean annual cycle in the same period in which the statistical model was fitted, namely 1960-1975. In this way the systematic errors of the climate model are subtracted out. The SLP patterns on which the two seasonal statistical models are based evolve differently in the Scenario A integration. This is shown in Figure 9, where the amplitudes of these patterns along the period of integration is depicted (to underline the low-frequency evolution the time series were seasonally averaged). The trends in all four cases are clearer from roughly the year 2050 onwards, where the effects of the additional greenhouse gas forcing should be more apparent. Concerning the winter SLP patterns, the amplitude of the first (second) SLP pattern (see Figure 2 tends to become more negative (positive) at the end of the integration, which means that the SLP contrast between the Asian continent and the Pacific Ocean tends to become weaker, leading to weaker winter Monsoon circulation. On the other hand the zonal circulation, represented by the second canonical pattern becomes more active in winter. In the summer season, the leading canonical pattern (see Figure 5) becomes stronger, which means that the westerlies over China in this season are weakened. Contrary to this, the more local pattern associated with the sea-level variability in the Yellow Sea gets stronger in the last decades of the integration, leading in this area to a more meridional (northerly) atmospheric circulation. It may be therefore concluded that in the future climate simulated by the ECHAM1-LSG model the atmospheric circulation over China will tend to be more zonal in the winter season and more meridional in the summer season. The estimated changes in sea-level at the three representative stations 5,8 and 12 (Fig 1) along the Chinese coast are shown in Figure 10. These estimations are obtained by applying the seasonal statistical models to the SLP Scenario A integration, separately for the winter and summer seasons. In order to show more clearly the long-term trends only the respective seasonal means are depicted in this figure, although these time series have been generated on a monthly basis. It can be seen that the estimated future changes are in general small, although one has to be aware that the changes originated in global thermal expansion of water and possible melting of glaciers have to be added up to those estimated by this statistical model,

Figure 9: *Seasonal amplitude of the different SLP patterns in the Scenario A integration. The SLP anomalies are referred to the simulated mean annual cycle in the period 1960-1975. The winter patterns are the canonical SLP patterns in figure 2. The summer pattern 1 is the canonical SLP pattern in figure 5 and the summer pattern 2 is the regression pattern in figure 6*



which are caused essentially by the action of wind-stress. Also of interest is the fact that the trends that are observed at the end of the integration may be of different signs for the winter and summer seasons, and for the stations located in the northern or southern stations. In winter the changes of sea-level seem to be negative in the South and positive in the Yellow Sea. In summer, on the other hand, the changes tend to be exactly opposite. This is due to the fact that the atmospheric circulation changes that are relevant for the coastal sea-level also tend to be opposite in summer with respect to the winter, as explained above. The sea-level in the stations located in intermediate positions are near zero on the long term.

## 6 Conclusions.

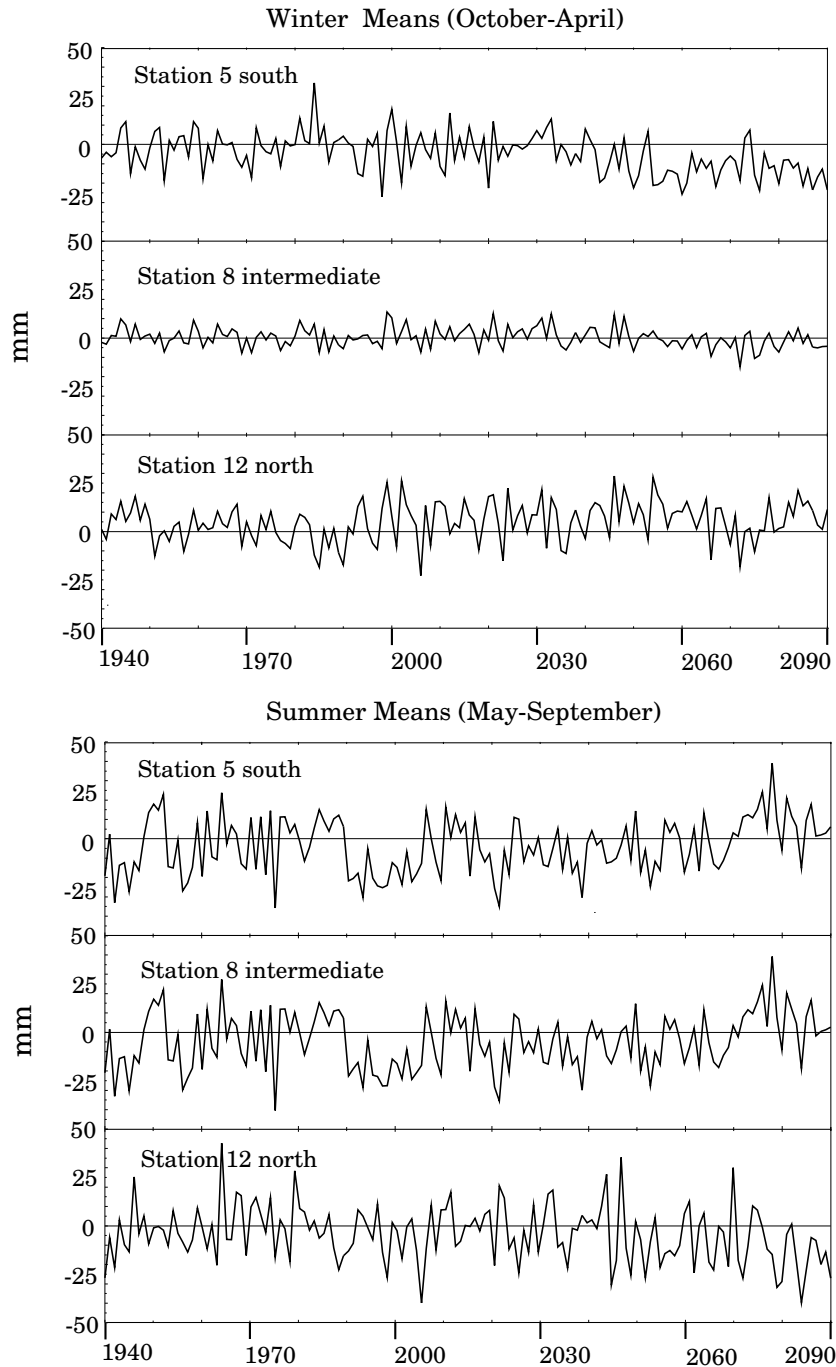
The relationships between the large-scale atmospheric circulation and coastal sea-level along the Chinese coast have been statistically analyzed. We have found that a great part of the sea-level variability may be explained generally by the intensities of the meridional and zonal atmospheric circulation over East Asia, although the optimal atmospheric patterns connected to sea-level variability are different for the summer and winter half years. The physical mechanism that explain these statistical relationships involve the direct piling up of seawater in the Yellow Sea and larger-scale Ekman pumping in the rest of the Chinese coast. The relationship of sea-level and SST is always weaker, so that we conclude that the steric effect plays a minor role in the coastal sea-level variability. A coupled atmosphere-ocean model integration forced by increasing atmospheric concentration of greenhouse gases according to the IPCC Scenario A has been analyzed in order to estimate the changes of the amplitudes of the relevant SLP patterns. It has been found that the atmospheric circulation over China by the year 2050 onwards tends to become more zonal in winter and more meridionally oriented in summer. The implied changes of coastal sea-level are estimated by means of the statistical model fitted with observed data. It is found that the sea-level changes are not very large (of the order of a few centimeters), and that the sign of the changes is opposite in winter and summer, and for the China Sea and for the Yellow Sea. This fact should be important in order to analyze long time series of coastal sea-level, either in this part of the world or elsewhere, to try to detect anthropogenic climate impact on sea-level. If our conclusions are confirmed the sea-level data should be seasonally stratified before undertaking such an analysis.

The IPCC 1995 estimation of mean global sea-level change under the Scenario A assumptions is 49 cm (IPCC, 1996), including the effects of water expansion, glacier melting and changes of the oceanic circulation. On the other hand the effect of changes in the intensity of local processes, such as storms, currents, waves, etc. is much more uncertain. If the results of the coupled climate model can be contribution of the atmospheric circulation through wind-stress will probably be not more important than the global factors in this part of the world.

*Acknowledgements.* This work was done during a visit of one of the authors, Prof. Cui, to

the Institute of Hydrophysics of the GKSS Research Centre in Geesthacht (Germany), that offered financial support and made this visit possible. The National Scientific Fund Committee of China and the Chinese Academy of Sciences contributed, through contract No. 49476274, to collect and pre-analyze the sea level data. H. von Storch helped us with valuable comments. U. Cubasch made the output of the coupled climate model available to us and K. Arpe kindly provided the sea surface temperature data.

Figure 10: *Estimated coastal sea-level changes along stations 5, 8 and 12 based on the statistical model linking SLP and sea-level and the SLP simulated by the ECHAM1-LSG coupled model forced by IPCC Scenario A greenhouse gas concentrations.*



REFERENCES

- Bretherton, C.S., C. Smith, and J.M. Wallace, 1992: An intercomparison of methods for finding coupled patterns in climate data. *J. Climate* **5**, 541-560
- Cayan, D., 1990. Variability of latent and sensible heat fluxes over the oceans. PhD thesis, University of California, San Diego.
- Chen X., 1991. Sea level changes since early 1920's from the long records of two tidal gauges in Shanghai. *Quaternary Coastline Changes in China*, 127-141, IGCP-274 China Working Group, Edited by Qin Yunshan and Zhao Zongling.
- Cubasch, U., K. Hasselmann, H. Höck, E. Maier-Reimer, U. Mijolajewicz, B. Santer, and R. Sausen, 1992: Time-dependent greenhouse gas warming computations with a coupled atmosphere-ocean model. *Clim. Dyn.* **8**, 55-69
- Cubasch, U., G. Hegerl, A. Hellbach, H. Höck, U. Mikolajewicz, B. Santer, and V. Boss, 1995. A climate change simulation starting at an early time of industrialization. *Clim. Dyn.* **11**, 71-84.
- IPCC, 1992: Climate Change: the supplementary report to the IPCC scientific assessment. J. Houghton, B.A. Callendar, S.K. Varney (eds). Cambridge University Press
- IPCC, 1996: Climate Change 1995- The science of climate change: Contribution of the Working Group I to the second Assessment Report of the Intergovernmental Panel on Climate Change. J.T. Houghton, L.G. Madeira Filho, B.A. Callander, N. Harris, A. Kattenberg and K. Maskell (eds). Cambridge University Press.
- Cui, M., H. von Storch, and E. Zorita, 1995: Coastal Sea level and the large-scale climate state: a downscaling exercise for the Japanese islands. *Tellus* **47A**, 132-144
- Gill, A., and P.P. Niiler, 1973 The theory of seasonal variability in the ocean. *Deep Sea Research* **20**, 141-177.
- Heyen, H., E. Zorita, and H. von Storch, 1996: Statistical downscaling of monthly mean North Atlantic air-pressure to sea-level anomalies in the Baltic Sea. *Tellus* **48A**, 312-323

- Lau, K-M, G.J. Yang, and S.H. Chen, 1988: Seasonal and intraseasonal climatology of summer Monsoon rainfall over East Asia. *Mon. Wea. Rev.* **116**, 18-37.
- Lau, N.-C., 1997: Interactions between global SST anomalies and the midlatitudes atmospheric circulation. *Bull. Amer. Meteor. Soc.* **78**, 21-33
- Lisitzin, E. and J. Patullo, 1961: The principal factors influencing the seasonal oscillation of sea level. *J. Geophys. Res.* **66**, 845-852
- Mikolajewicz, U., B. Santer and E. Maier-Reimer, 1990: Ocean response to greenhouse gas warming. *Nature* **345** 1-5.
- Patullo, J., W. Munk, R. Revelle, and E. Strong, 1955: The seasonal oscillation in sea level. *J. Marine Research* **14**, 88-155.
- Tao, S-Y, and L.X. Chen, 1987: A review of recent research on the East Asian summer Monsoon in China. In *Monsoon Meteorology*, C.P. Chang and T.N. Krishnamurti (eds). Oxford University Press 60-92.
- Sahagian, D., F. Schwartz, and D. Kakobs, 1994: Direct anthropogenic contribution to sea-level rise in the twentieth century. *Nature* **367**, 54-57 .
- von Storch, H., E. Zorita, and U. Cubasch, 1993: Downscaling of global climate change estimates to regional scale: an application to Iberian rainfall in wintertime. *J. Climate* **9** 1161-1171.
- Wang, S-W, and Z-C Zhao, 1981: Droughts and floods in China 1470- 1979. In *Climate and History*, T.M. Wigley, M.I. Ingraham and G. Farmer (eds), Cambridge University Press, 271-288
- Warrick, R.A., and H. Oerlemans, 1990: Sea level rise. In *Climate Change. The IPCC Scientific Assessment*. Hought, Jenkins, and Ephraum (eds). Cambridge University Press.
- Wunsch, C., and D. Stammer, 1997: Atmospheric loading and the inverse barometer effect. *Rev. of Geophys.* **35**, 79-107
- Wyrtki, K. , 1990: Sea level rise: the facts and the future. *Pacific Science* **44** 1-16.